



# Discrimination of Iron High Potential Zones at the Zaghia Iron Ore Deposit, Bafq, Using Index Overlay GIS Method

Behnam Sadeghi<sup>\*1</sup>, Masoumeh Khalajmasoumi<sup>2,3</sup>, Peyman Afzal<sup>4,5</sup>, Parviz Moarefvand<sup>6</sup>

1. Department of Earth and Oceans, James Cook University, Townsville, Queensland 4811, Australia

2. Department of Geology, Islamic Azad University, Science and Research Branch, Tehran, Iran

3. Applied geological research center, Geological Survey of Iran, Iran

4. Department of Mining Engineering, Faculty of Engineering, South Tehran Branch, Islamic Azad University, Tehran, Iran

5. Camborne School of Mines, University of Exeter, Penryn, UK

6. Department of Mining Engineering, Amirkabir University of Technology, Tehran, Iran

Received 16 February 2014; accepted 10 September 2014

## Abstract

GIS is considered an important technique as well as a prerequisite for cost effective mineral exploration and determination of high potential areas. The purpose of this research is to determine high potential iron zones for detailed exploration using index overlay GIS method. Index Overlay was used to combine the geology, topography (scale: 1:1,000), lineaments, remote sensing (ASTER and ETM+) and geochemical data. Appropriate weights were allocated to each layer based on the significance of each data layer. Concentration-area fractal method was applied to data acquired from trenches in order to isolate iron anomalies and add them to the geochemical layer. Evaluation of the information layers along with fractal analysis, differentiated three geochemical iron populations. By combining the information layers obtained from GIS, high potential zones were determined. Regions with codes 1, 2 and 3 are the most promising areas, respectively, and are proposed for more detailed exploration and drilling.

**Keywords:** Zaghia, fractal, concentration-area, iron mineralization, index overlay

## 1. Introduction

In weak anomalies, which are related to mineral deposits, one information layer is not sufficient; several accurate information layers are needed [1, 2, 3, 4]. One of the applications of the Geographic Information System (GIS) as a georeferencing system in mineral exploration is the provision of an appropriate environment for importing, analyzing and modeling a large amount of data. Using this system, data can be evaluated simultaneously and propose the best areas to explore. The Zaghia iron deposit, anomaly 2C, is located 120 km east of Yazd, approximately 15 km east of Bafq in Yazd province and 12 km south-east of the Choghart iron mine (Fig1). It is situated in the Esfordi 1:100,000 scale mapping sheet.

Exploratory studies of Zaghia, anomaly 2C, began in the Bafq-Zarand block using airborne magnetometry. Systematic exploration was performed between 1969-1977 using ground magnetometry, gravimetry and core drilling. A 1:100,000 scale geological map of Zaghia was created after which magnetometry operations were done at the same scale [5]. Detailed explorations, carried out by IMPASCO, consisted of 31 boreholes and 4 trenches (Fig1).

## 2. Geological Setting of the Zaghia Iron Ore Deposit

According to field geology observations and mineralogical data obtained from four trenches, particularly in the southeastern portion of the deposit (Fig1, 2), most of the studied area is covered by alluvium and contains small mineralized outcrops on the surface. The maximum and minimum heights of the study are 1,249 m and 1,114 m respectively. Morphologically, the deposit consists of two units, alluvial sediments and semi mountainous areas. A majority of the study area consists of flat, alluvial, Quaternary period sediments. The alluvial sediments are traversed by NW-SE and NE-SW flowing streams. The deposit is bordered by the Narigan Mountains to the east [5]. According to the lithological model of the deposit, generated by RockWorks v.15, high grade mineralization of Fe occurs at the surface as well as the central portion of the deposit with a large portion of the area consisting of schist and limestone [5, 6, 7, 8].

## 3. Concentration -Area Fractal Method

In recent years, fractal methods have been widely accepted due to their ability to analyze raw data [9]. Concentration-area (C-A) fractal method, considering the concentration factor, can provide efficient results in the determination of populations and alteration zones. Cheng et al. (1994) proposed a new methodology

\*Corresponding author.

E-mail address (es): behnam.sadeghi@my.jcu.edu.au

based on multi-fractal geochemical distribution to demonstrate the experimental and practical connections

between concentration and area [10, 11, 12, 13, 14, 15, 16].

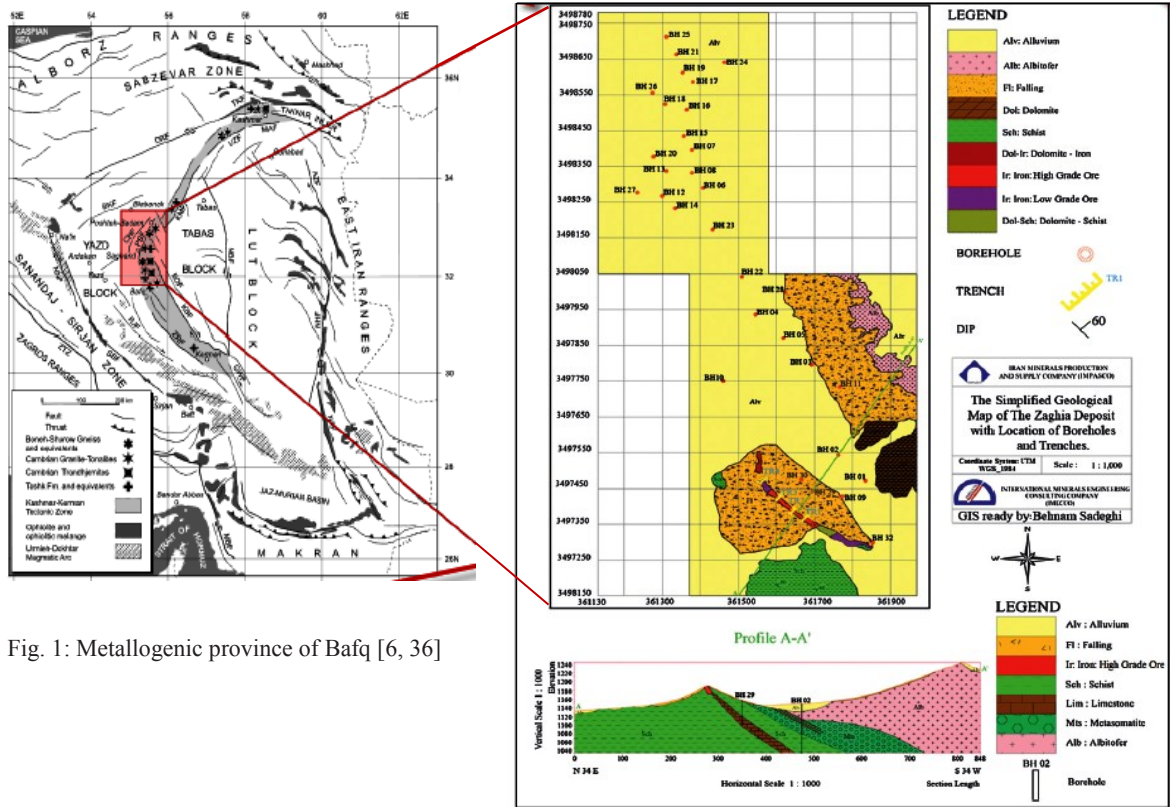


Fig. 1: Metallogenic province of Bafq [6, 36]

For the studied area, the C-A method was based on the area occupied by a specific concentration as well as the correlation between the power law parameter  $M(\delta)$  and under evaluation parameter  $(\delta)$ . The model is expressed by the following equation:

$$(1) \quad M(\delta) \propto \delta^{-\alpha}$$

In this equation,  $\delta$  denotes element concentration and  $\alpha$  represents the fractal dimension of the distribution of element concentrations [6, 17]. This method is used to explain the relationship between geological, geochemical and mineralogical results and information. The most useful feature of this method is its ability to separate geochemical anomalies from the background using thresholds [10, 18]. This method can be used to describe patterns and classify images based on C-A diagrams [10, 12, 13, 19]. The general equation which is proposed by Cheng et al. is [10, 15, 18, 20]:

$$(2) \quad A(\rho \leq v) \propto \rho^{-a_1} ; A(\rho \geq v) \propto \rho^{-a_2}$$

In this equation,  $\rho$  denotes element concentration,  $a$  denotes the fractal dimension of the distribution of element concentrations and  $v$  represents the threshold amounts.

The basis of these two equations is the distribution function proposed by Evertz and Mandelbrot (1992). This function shows the correlation between the measurements of 2D cells and 3D voxels with their amounts and measured parameters [18]. The distribution function is expressed by the following equation:

$$(3) \quad \chi_q(\varepsilon) = \sum_{i=1}^{N(\varepsilon)} \mu_i^q$$

In this equation,  $\chi_q$  denotes the distribution function,  $\varepsilon$  denotes the measurements of 2D cells, 3D voxels or generally measured elements and  $\mu$  denotes the measured parameter of each element [17].

#### 4. Methodology

The index overlay method is a knowledge-based modeling method. Knowledge-based methods are appropriate in the beginning stage of exploratory operations, especially in areas with a lack of information. These methods are used in areas where there are no known resources or where resources are scarce (Green Fields) [1, 2]. Index overlay consists of two methods [3]. In each method expert observations and the importance of the effective factors are considered in order to recommend information layer weights. These weights are positive integers or real

numbers within a specified range. In the first method, the input maps are binary and have single weighting factors. To combine this information with other maps the weight factor and the importance of different classes in the factor map are the same and should be multiplied. The second method is more flexible. In

addition to assigning weights to each layer, each class and location unit of each factor map is given a weight. In this approach processors classify the information layers according to their knowledge and assign an appropriate weight to each layer.

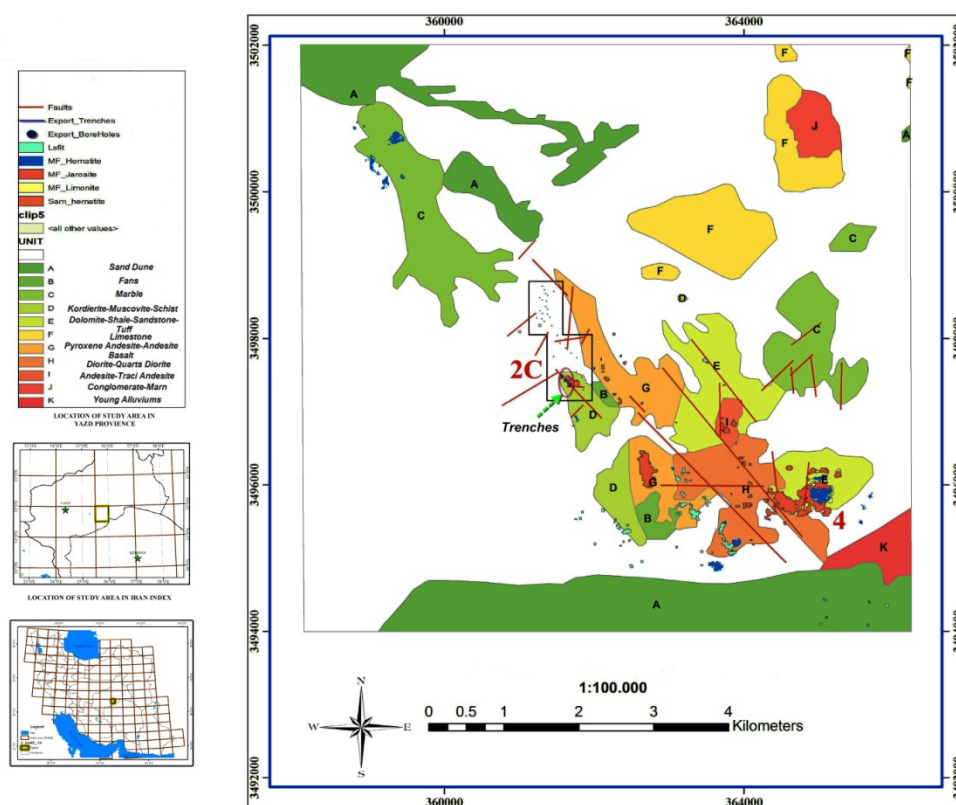


Fig. 2: Geological map of Zaghia iron ore deposit [6]

The average value of each part of the final layer, a combination of all the layers, is obtained using the following formula [1, 2, 6]:

$$(4) \quad \bar{S} = \frac{S_{ij}W_i}{W_i}$$

In this formula  $\bar{S}$  denotes the weight value of each layer,  $W_i$  denotes the layer weight, and  $S_{ij}$  denotes the weight of the class  $i$  in the layer  $j$ . This method has been used by other researchers as well (e.g. [4, 21, 22, 23]). One of the advantages of this method is that it allows for uncertainty.

## 5. Generation of Information Layers for Study Area

### 5.1. Geological and Topographical Maps

After reviewing 1:5,000 scale topographic and geologic maps, the most suitable mineralization areas

were selected. Topographic and geologic maps at 1:1,000 scale were then generated. A 50 hectare area was selected and a topographic map was initiated using Thales single frequency GPS. After selecting a rectangular area located in zone 40, the XYZ points were measured using the UTM-WGS84 system. All natural and non-natural features such as topography, roads, trenches lithological units, faults, slopes and tension of the beds were recorded.

The Zaghia iron deposit, anomaly 2C, is located in the Bafq block of central Iran. This block is a horst extending from Kerman to Bafq, Saghand and Robate Poshtebadam. This block follows a north-west trend similar to that of the Kuh Banan fault to the east and Kuh Daviran fault to the west. The classification of the geological units of the Bafq block is based on a 1:250,000 scale geological map prepared by German geologists from 1960 to 1961 as well as 1:100,000

scale geological maps of Esfordi and Bafq provided by Geological Survey of Iran. Information pertaining to the exploration operations was obtained by the geologists of National Steel Co. [5] (Fig1, 2).

Due to a broad alluvial cover in the area only a few outcrops in the southeastern portion of the deposit were observed through an on sight visit and the use of a 1:5,000 scale map of the area. Based on this information four trenches were excavated (Fig2) revealing magnetite with volcanic Kiruna host rock. These units were separated and used in the GIS combination. Due to its importance this layer was given a weight of 50 [24].

**5.2. Lineaments Layer**

Because mineralization along lineaments is more probable, lineaments are considered one of the most significant factors involved in mineralization, especially in iron deposits [5, 25]. The map of the lineaments in the area was generated using a geological map of the area and remote sensing data. The mineralization and faults, including minor faults to the northeast, mainly follow a NW-SE trend. The plotted rose diagram displays the trends of the faults in the area (Fig4). A 90 meter buffer along with a weight of 10 was assigned to this layer (Fig2, 3).

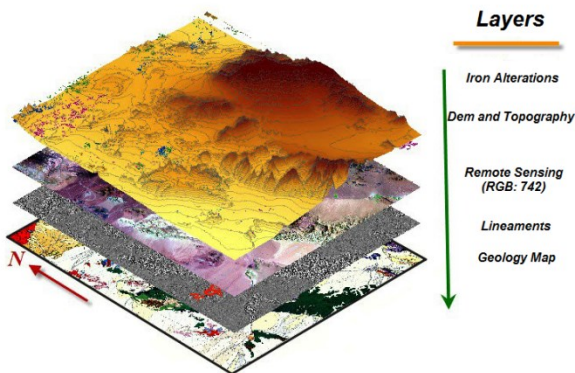


Fig. 3: Schematic map of all primitive information layers

**5.3. Geochemical Layer of Trenches**

After creating a 1:5,000 scale geological map and selecting suitable locations for generating additional maps at 1:1,000 scale, four trenches (approximately 110 meters long) were chosen. The iron outcrops of the trenches were excavated in order to determine the lower and upper limits and obtain samples from the non-weathered units of the area. Due to the fact that only a small number of samples were able to be obtained and geochemical results revealed that the iron in the trenches was exposed, this layer was given a weight of 5.

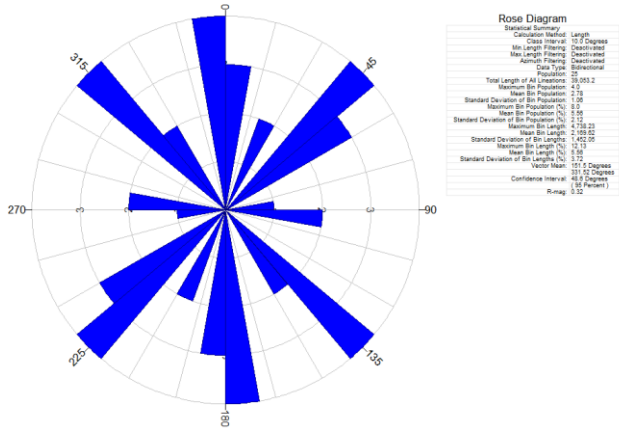


Fig. 4: Rose diagram of lineaments of the area

**5.4. Alteration Layer Acquired From Remote Sensing Data**

In recent years remote sensing has provided valuable information in the area of mineral exploration. Satellite data has been broadly used in geology and mineral exploration to record the results of photography in the electromagnetic spectrum. The geological structures of the study area, lithology types and alterations are important extractable layers obtained using satellite images [6, 7, 26, 27, 28, 29, 30]. Lithological evaluations have two vital goals; the discovery and identification of lithological units on a regional scale as well as concentration levels of specific minerals in the area. Based on photo interpretation, multi-spectral data is more useful when used in the appropriate scale. Satellite image processing and the absorption characteristics of the bands were used to identify mineral concentrations [26]. Different algorithms were used to excavate the most common alterations in the area such as iron-oxide, actinolite and diopside [31]. A comparison of remote sensing algorithms showed that Linear Band Prediction (LS-Fit) and Band Ratio (3/1 and 2/1) methods yield the best results for the delineation of iron-oxides while Matched Filtering (MF) method yielded the best results when evaluating actinolite and diopside alterations [30]. The weights of 20, 10 and 5 were given to the iron-oxide, actinolite and diopside alterations, respectively.

**5.5. Concentration-Area (C-A) Fractal Method**

The surface data taken from the trenches was analyzed using C-A fractal method in order to distinguish the superficial geochemical anomalies of the deposit. The local distribution of the concentrations was estimated using Inverse Distance Weighted (IDW) method. According to the logarithmic diagram, two breakpoints displaying concentration borders among mineralization zones and wall rock were recognized. These breakpoints are thresholds measuring 1.24 and 1.65. Thus, three populations were separated. The

concentrated Fe anomalies showed values higher than 44.7%. Low grade Fe anomalies were between 17.4 % - 44.7%, while Fe values lower than 17.4% illustrate the background. This log-log plot shows a multi-fractal model (Fig5). Based on these results, an Fe distribution map was generated using RockWorks v15 and was

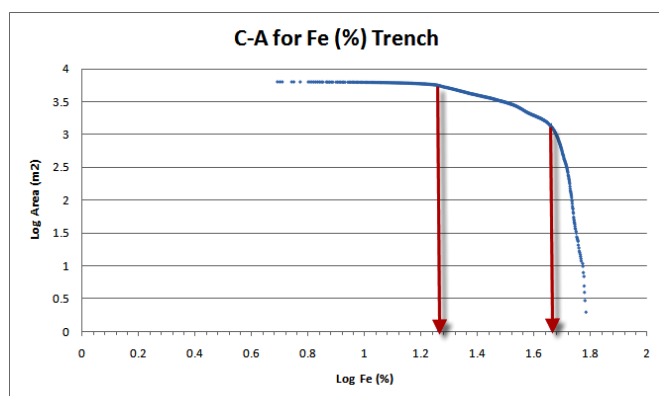


Fig. 5: Multi-fractal diagram of trench data

juxtaposed with other geological observations (Fig6). This layer is a subset of the geochemical layer. The final histogram displays the three populations resulting from the C-A method (Fig7) [14, 19, 32, 33, 34, 35].

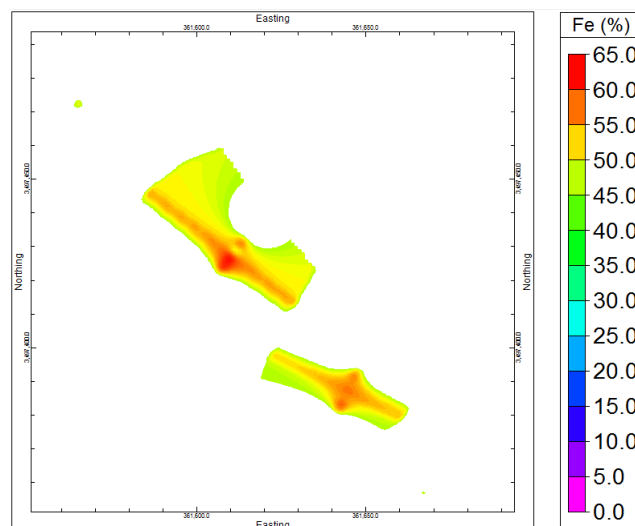


Fig. 6: Final map obtained using C-A method

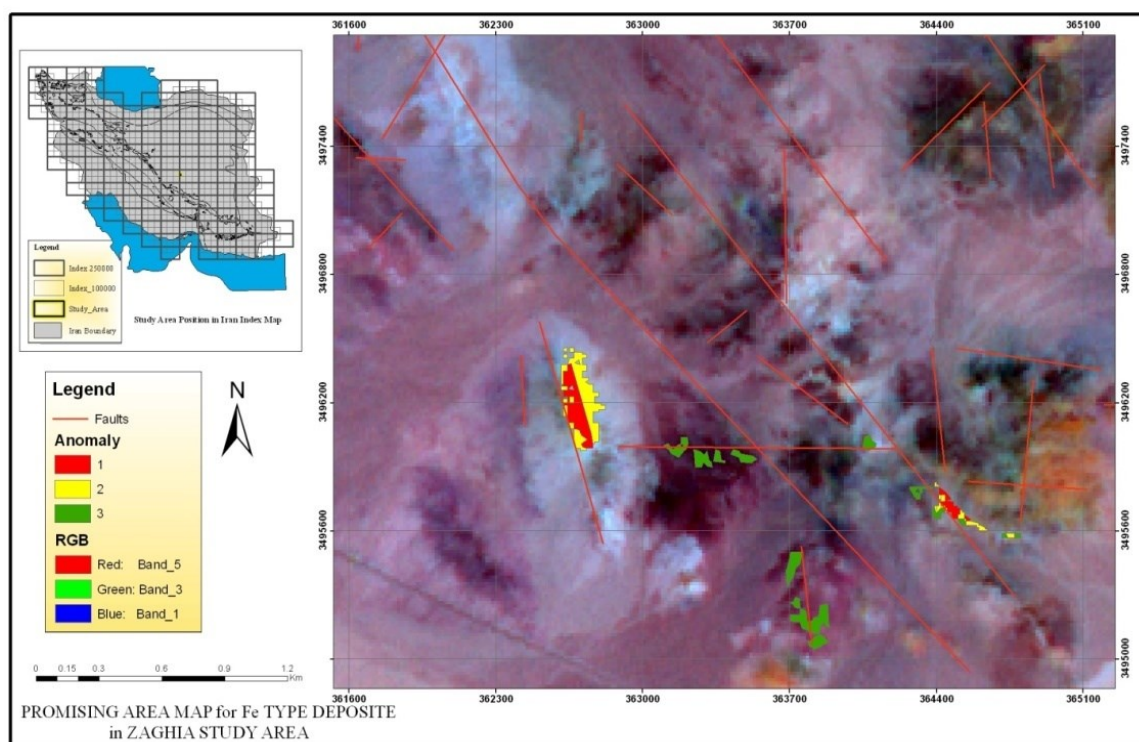


Fig. 8: Final map of the description model of the deposit with the extracted structures from ETM+ satellite images (e.g. RGB: 531); grade one, two and three anomalies are shown.

## 6. Combination of All Information Layers

Possible iron mineralization types were selected considering geological conditions, probable ore deposit

types and mineralization patterns in the region. Using USGS models, geological units of each type of mineralization were separated from a geological map

of the area based on descriptions of each type of mineralization. Then, combination and modeling were carried out based on alterations using satellite image processing and the effective processes of mineralization consisting of geochemical guides, trends of local and regional structures and lineaments. Each of these factors was included in the combination and given a specific importance factor according to mineralization type [31]. All data processing steps,

combination and modeling were done using GIS. The layers of the geology, lineaments, geochemistry (of trenches and C-A fractal model) and alterations (iron oxides, diopside and actinolite), obtained using remote sensing, were utilized in the combination and given the weights of 50, 10, 5, 5, 20 and 10 respectively (Fig8, 9).

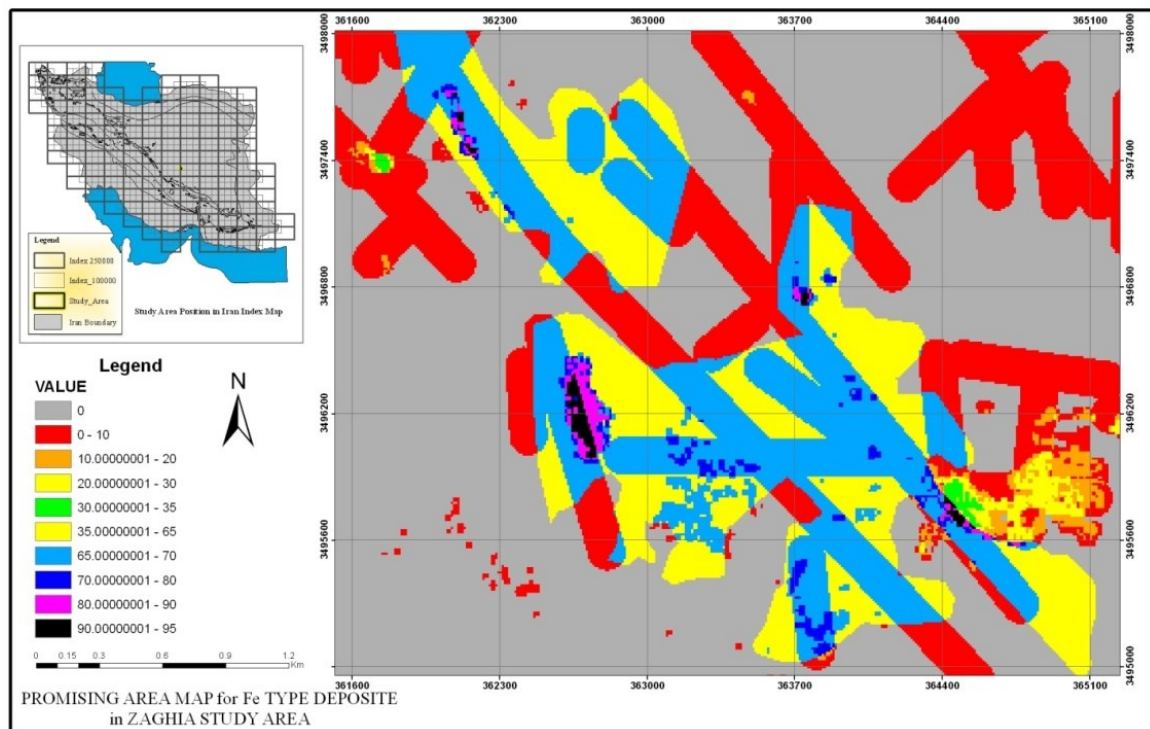


Fig. 9: General map of the description model of the deposit showing the possible percentage of iron mineralization. Black and pink areas represent potential iron mineralization.

## 7. Conclusions

Combination and modeling based on the integration of information from all layers (geology, geochemistry, fractal model and remote sensing data), were performed in a GIS environment using Arc map v.10.2 software. On the basis of the final combined model three high potential areas were identified and should

be considered for more detailed exploration.

## Acknowledgements

The authors would like to thank the reviewers for their valuable input and Dr. Behzad Mehrabi for his assistance and guidance.

## References

- [1] Carranza, E.J.M., 2008, Geochemical anomaly and mineral prospectivity mapping in GIS, Handbook of Exploration and Environmental Geochemistry: Elsevier, Amsterdam.
- [2] Yousefi, M. and Kamkar Rouhani A., 2010, Principle of Mineral Potential Modeling Techniques (In Geographical Information System): Amirkabir University of Technology Press, Tehran.
- [3] Bonham-Carter, G.F., 1994, Geographic information systems for geoscientists: modeling with

GIS: Pergamon, Oxford.

- [4] Harris, J.R., Wilkinson, L., Heather, K., Fumerton, S., Bernier, M.A., Ayer, J. and Dahn, R., 2001, Application of GIS Processing Techniques for Producing Mineral Prospectivity Maps– A case study: mesothermal Au in the Swayze Greenstone Belt, Ontario, Canada: Natural Resources Research, v. 10, p. 91– 124.

[5] IMECCO, 2010, General Exploration of Zaghia (IIC) Iron Ore Deposit Report, International Minerals Engineering Consultant Company (IMECCO).

- [6] Sadeghi, B., 2012, Application of Concentration-Number fractal method to outline of mineralized zones in the Zaghia iron ore deposit, Bafq, anomaly 2C. M.Sc thesis, Islamic Azad University, South Tehran branch, Tehran, Iran (In Farsi with English abstract).
- [7] Sadeghi, B., Moarefvand, P. and Afzal, P., 2010, Determination of Fe grade distribution using concentration-number fractal method in boreholes of Zaghia iron ore deposit, Bafq: Journal of Earth and Resources, 2012a, v. 12, p. 51-60.
- [8] Sadeghi, B., Moarefvand, P., Afzal, P., Yasrebi, A.B. and Daneshvar Saein, L., 2012, Application of fractal models to outline mineralized zones in the Zaghia iron ore deposit, Central Iran: Journal of Geochemical Exploration, v. 122, p. 9-19.
- [9] Mandelbrot, B.B., 1983, The Fractal Geometry of Nature: W. H. Freeman, San Francisco.
- [10] Cheng, Q., Agterberg, F.P. and Ballantyne, S.B., 1994, The separation of geochemical anomalies from background by fractal methods: Journal of Geochemical Exploration, v. 51, p. 109-130.
- [11] Cheng, Q., 1997c, Multifractal modeling and spatial analysis, In: Glahn, V.P. (Ed.): Proceedings, IAMG'97 meeting, Barcelona, Spain, v. 1, p. 57-72.
- [12] Cheng, Q., 1999, Spatial and scaling modelling for geochemical anomaly separation: Journal of Geochemical Exploration, v. 65 (3), p. 175-194.
- [13] Cheng, Q., 1999a, Multifractality and spatial analysis: Computer and Geosciences, v. 25, p. 949-961.
- [14] Cheng, Q., 1998, Spatial and scaling modeling for image analysis. In: Buccianti, A., Nardi, G., Potenza, R. (Eds.): Proceedings of the Four Annual Conference of the International Association for Mathematical Geology, Ischia, Italy, v. 2, p. 713-718.
- [15] Goncalves, M.A., Vairinho, M. and Oliveira, V., 1998, Study of geochemical anomalies in Mombeja area using a multifractal methodology and geostatistics. In: Buccianti, A., Nardi, G., Potenza, R. (Eds.): Proceedings of International Association for Mathematical Geology Meeting, Ischia, Italy, v. 2, p. 590-595.
- [16] Sim, B.L., Agterberg, F.P. and Beaudry, C., 1999, Determining the cut of between background and relative base metal smelter contamination levels using multifractal methods: Computer and Geosciences, v. 25, p. 1023-1041.
- [17] Afzal, P., 2010, Demonstration of Zone detection model in porphyry deposits by using 3D fractal methods, Case study: Kahang Copper porphyry, Isfahan. Unpublished Ph.D thesis, Islamic Azad University, Science and Research branch, Tehran, Iran (In Farsi with English abstract).
- [18] Li, C., Ma, T. and Shi, J., 2003, Application of a fractal method relating concentrations and distances for separation of geochemical anomalies from background: Journal of Geochemical Exploration, v. 77, p. 167-175.
- [19] Cheng, Q. and Li, Q., 2002, A fractal concentration-area method for assigning a color palette for image representation: Computer and Geosciences, v. 28, p. 567-575.
- [20] Mehrnia, R., 2009, Using Fractal Filtering Techniques For Processing ETM Data As Main Criteria For Evaluating Of Gold Indices In North West Of Iran: International Conference on Computer Technology and Development.
- [21] De Araujo, C.C. and Macedo, A.B., 2002, Multicriteria Geologic Data Analysis for Mineral Favorability Mapping: Application to a metal Sulphide Mineralized Area, Ribeira Valley Metallogenic Province, Brazil: Natural Resources Research, v. 11, p. 29-43.
- [22] Chica-Olmo, M., Abarca, F. and Rigol, J.P., 2002, Development of a Decision Support System Based on Remote Sensing and GIS Techniques for Gold-rich Area identification in SE Spain: International Journal of Remote Sensing, v. 23, p. 4801-4814.
- [23] Billa, M., Cassard, D., Lips, A.L.W., Bouchot, V., Turlere, B., Stein, G. and Guillou-Frottier, L., 2004, Prospecting Gold-rich Epithermal and Porphyry Systems in the Central Andes with a Continental-Scale Metallogenic GIS: Ore Geology Reviews, v. 25, p. 39-67.
- [24] Hassanipak, A.A. and Shojaat, B., 2001, Ore Deposit Modelling (Metallic & Nonmetallic) with Exploration Approach: Tehran University Press, Tehran.
- [25] Fathianpour, N., Ghaedrahmati, R. and Hazeri, M., 2009, Discrimination of parts bearing high potential of Pb-Zn at Irankoh region in Isfahan in GIS environment: IRANIAN JOURNAL OF MINING ENGINEERING, v. 8, p. 13-22.
- [26] Sabine, C., 1999, Remote sensing strategies for mineral exploration. In: Rencz A. (ed.) Remote sensing for the earth sciences- Manual of remote sensing: American Society of Photogrammetry and Remote Sensing, p. 375-447.
- [27] Sabins, F.F., 1999, Remote sensing for mineral exploration: Ore Geology Reviews, v. 14, p. 157-183.
- [28] Babaei, K. and Sadeghi, B., 2010, Discrimination of alteration zones from ASTER SWIR data in the lead and zinc abandoned area of RoknAbad in Ardabil province: International Mining Congress & Expo, Tehran, Iran.
- [29] Khalajmasoumi, M., Shahhosseini, A., Bayatani, A. and Eyne, A., 2010, Identification of uranium mineralization by processing ASTER images, Hamedan: 29th Earth Science Congress, Tehran, Iran.
- [30] Sadeghi, B., Khalajmasoumi, M., Afzal, P., Moarefvand, P., Yarebi, A.B., Wetherelt, A., Foster, P. and Ziazarifi, A., 2013, Using ETM+ and ASTER sensors to identify iron occurrences in the Esfordi 1:100000 mapping sheet of Central Iran: Journal of

African Earth Sciences, v. 85, p. 103-114

[31] Alavipanah S.K., 2003, Application of Remote Sensing in the Earth Sciences (Soil): University of Tehran Press, Tehran.

[32] Cheng, Q., 1994, Multifractal modeling and spatial analysis with GIS: gold potential estimation in the Mitchell- Sulphurets area, Northwestern British Columbia: Ph.D thesis, Dissertation, University of Ottawa, Ottawa.

[33] Harris, J.R., Rencz, A.N., Ballantyne, S.B. and Sheridan, C., 1998, Mapping altered rocks using LANDSAT TM and lithochemical data: Sulphurets-Brucejack Lake district, British Columbia, Canada: Photogrammetric Engineering and Remote Sensing, v. 64 (4), p. 309-322.

[34] Rencz, A., Harris, J. and Ballantyne, S.B., 1994, LANDSAT TM imagery for alteration identification: Geological Survey of Canada, p. 277-282.

[35] Sadeghi, B., Afzal, P., Moarefvand, P. and Khoda Shenasi, N., 2012, Application of Concentration-Area fractal method for determination of Fe geochemical anomalies and the background in Zaghia area, Central Iran: 34th International Geological Congress (IGC), Brisbane, Australia.

[36] Ramezani, J. and Tucker, R.D., 2003, The Saghand region, Central Iran: U-Pb Geochronology, Petrogenesis and Implications for Gondwana Tectonics: American Journal of Science, v. 303, p. 622-665.